Modeling and Simulation of Bearingless Switched Reluctance Motor in Full-Period Generating Mode Based on Matlab

Zhuang Zheng[1,a], Deng Zhiquan[1,b], Cao Xin[1,c], Yao Tian[1,d], Zhou Qin[1,e], Fan Na[1,f]
[1]Nanjing University of Aeronautics and Astronautics, Nanjing, 210016, China
[a]kensouzh@yahoo.com.cn, [b]dzq@nuaa.edu.cn,
[c]cxxc118@nuaa.edu.cn,[d]yxg2002@yahoo.com.cn, [e]qin_chou@163.com,
[f]fanna_065@yahoo.com.cn

Abstract: In this paper, the model of bearingless switched reluctance motor in full-period generating mode is established using relative blocks of MATLAB/SIMULINK. The validity of simulation model is tested and verified through the derived waveform without considering levitation force. The model is simulated to analyze the influence of chopper current and speed on output voltage. Relations between radial forces and winding currents are studied from the simulation results.

Keywords: Bearingless, Switched Reluctance Generator, Modeling

Introduction

Bearingless switched reluctance motors (BSRM), which have combined characteristics of switched reluctance motors (SRM) and magnetic bearings, could control rotor radial positions with magnetic pulls. BSRM effectively solves the problem of bearing abrasion which could fully enhance motor's high-speed performance [1,2].

Switched reluctance generator (SRG) only has one winding on the stator. The winding is used for both excitation and generation which limits the output power. Compared with SRG, full-period bearingless switched reluctance generator (FPBSRG) has two windings on the stator. One winding is called as radial force winding and the other is main winding. The radial force winding is used for excitation and levitation force generated. The main winding is only used for generation. FPBSRG reinforce excitation which could enhance the output power [3].

The design and analysis of FPBSRG are difficult because of its dual-salient structure and the coupling of windings. The usage of MATLAB/Simulink makes the calculation convenient, the interface clear, and the information plenty fullness. It is an ideal environment for stable simulation models. In this paper, the linear simulation model of FPBSRG is established using relative blocks of MATLAB/SIMULINK. Then the model is simulated to analyze the characteristics of the generator.

Principle of FPBSRG

Fig.1 shows the A-phase winding configuration of a 12/8 FPBSRG. The motor main winding, which consists of four coils connected in series, is connected to a rectifier bridge. On the other hand, the radial force winding consists of only one coil. Each coil is controlled

independently.

Fig.2 shows the principle of radial force production. The thick solid lines show the fluxes produced by both the main winding and the radial winding. When the radial-force winding N_{sa1+} current is increased, it is evident that the flux linkage in air-gap 1 is increased. Therefore, this superimposed magnetic field results in the radial force F acting on the rotor towards the positive direction of α axis. If the current of N_{sa1-} is larger than that of N_{sa1+}, the radial force F will act towards the negative position of α axis. Moreover, a radial force in the β axis can be produced by the radial force winding current in β axis. Thus, radial force can be produced in any desired direction. Similarly, this principle can be suitable for the other two phases. The motor can achieve stable suspension if each radial winding current is controlled properly.

Fig.3 shows the typical current waveforms of FPBSRG. When the radial-force winding is turn-on, the exciting current rises. The flux linkage rises till the rotor reaches the aligned position of rotor and stator poles. The main winding generates current to decrease the change of flux linkage due to flux-weakening. When the radial-force winding is turn-off, the flux linkage decreases due to the reduction of the phase inductance and exciting current. At this moment, electric power is generated in the main winding which is similar to the theory of conventional SRG. In this mode the main winding can provide power in full period.

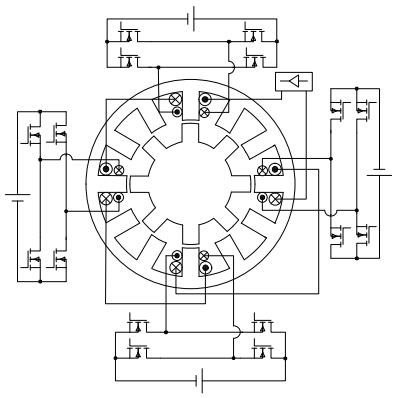

Fig.1 A-phase configuration of a 12/8 FPBSRG

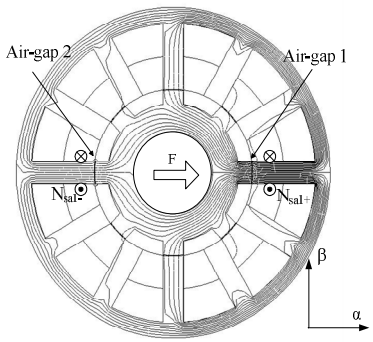

Fig.2 Principle of radial force production

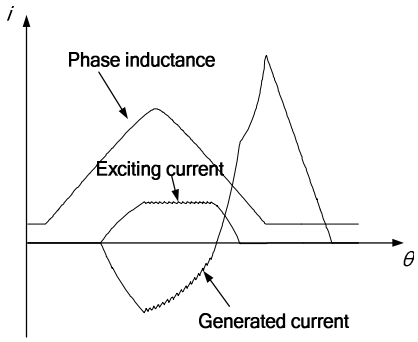

Fig.3 Typical current waveforms of FPBSRG

The Model Establishment of FPBSRG

The FPBSRG system consists of a 12/8 bearingless switched reluctance motor, a digital control system, a inverter for radial-force winding, a rectifier bridge for main winding, a position detecting circuit and a current detecting circuit. To simplify the analysis, some assumptions are made as follows:

(1) The switch elements and diodes have no transient processes when turned on or turned off. The voltage drops of these elements are zero.

(2) The inductances of three phases are symmetric. The phase-to-phase mutual inductances

of the main winding and the mutual inductances between the main winding and radial-force winding are small enough to be ignored.

(3) The rotating speed is constant.

(4) The magnetic circuit is not saturated.

(5) The resistance of main winding and radial-force winding are not considered.

The schematic diagram of the simulation model is shown in Fig.4. The model consists of several specific-function modules: the angle control module, the inductance assignment module, the radial-force-winding control module, the main winding module, the radial-force calculation module, etc.

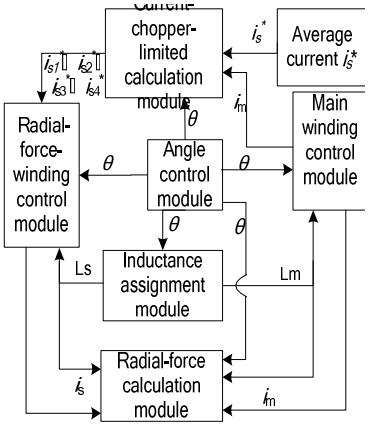

Fig.4 Schematic diagram of FPBSRG simulation model

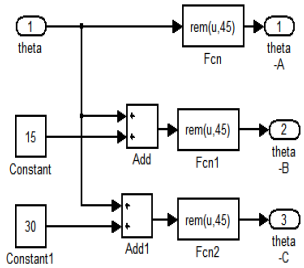

Fig.5 Angle control module

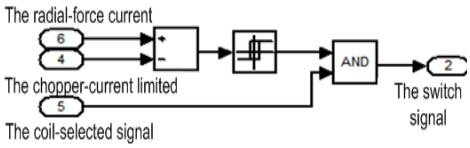

Fig.6 Chopper module

Fig.5 shows the angle control module which is used to calculate the angles of each phase. The phase inductance period is 45º as the structure of the motor is 12/8. The phase differential is 15º. A 45º remainder module is adopted as shown in the figure.

The inductance assignment module assigns the value of inductance. The inductance can be looked up in the inductance table when the angle changes.

Fig.6 displays the chopper module of the radial-force winding. The current-chopper limited is given from the current-chopper-limited calculation module as shown in Fig.7. The chopper band-width can be modified by changing the parameter of the hysteresis module.

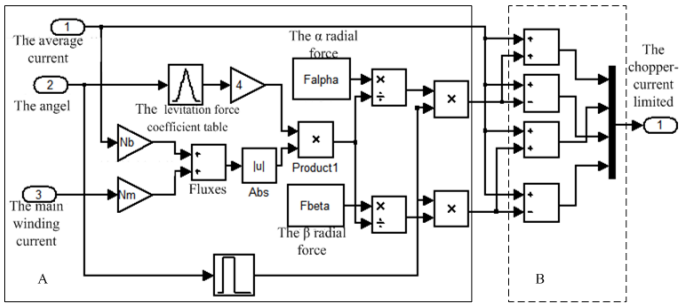

Fig.7 Current-chopper-limited calculation module

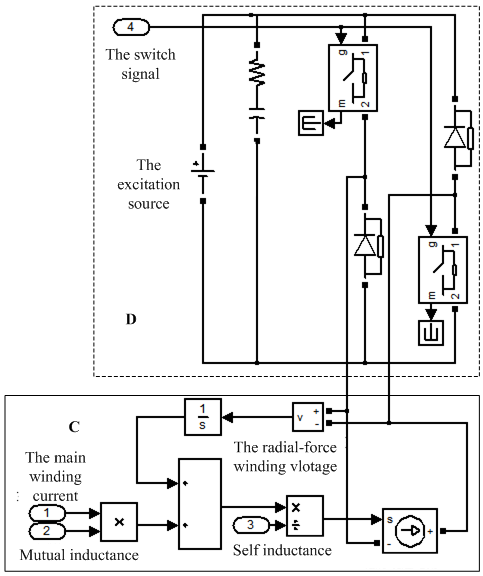

Fig.8 Radial-force-winding control module

The current-chopper-limited calculation module is used to calculate the current-chopper limited of four radial-force-winding coils (i_{s1}*, i_{s2}*, i_{s3}*, i_{s4}*). To achieve suspension, the calculation algorithm is as follows:

The levitation force equations can be written as,

$$F_\alpha^* = 4K_f(\theta)\left[N_b i_s^* - N_m i_m\right]\Delta i_{s1}^* \tag{1}$$

$$F_\beta^* = 4K_f(\theta)\left[N_b i_s^* - N_m i_m\right]\Delta i_{s2}^* . \tag{2}$$

Here, $K_f(\theta)$ presents the levitation force coefficient, and N_m, N_s are the turns of the main winding and radial-force winding, respectively. Then, i_{s1}*, i_{s2}*, i_{s3}*,and i_{s4}* can be calculated from the relational expressions $\triangle i_{s1}^* = |i_{s1}^* - i_{s3}^*|/2$, $\triangle i_{s2}^* = |i_{s2}^* - i_{s4}^*|/2$ and $i_s^* = (i_{s1}^* + i_{s3}^*)/2 = (i_{s2}^* + i_{s4}^*)/2$.

The inputs of the current-chopper-limited calculation module are the angles of the rotor θ, the average current value i_s*, and the radial force F_α*, F_β*. The solid line box A computes $\triangle i_{s1}$ and $\triangle i_{s2}$*. Then the dotted box B calculates i_{s1}*, i_{s2}*, i_{s3}*and i_{s4}* from the results of box A.

The radial-force-winding control module can be divided into two parts, solid line box C and dotted box D, as shown in Fig.8. Box C calculates the currents and voltages of the radial-force winding. Box D is the power circuit which is an asymmetrical half-bridge. The switch signals are given from the chopper module. The two main switches of one coil use the same switch signal.

The voltage equations of the main windings and the radial-force windings can be

written as,

$$-U_m = i_m r_m + \frac{d\psi_m}{dt} - \sum_{n=1}^{4} \frac{d\psi_{msn}}{dt} \tag{3}$$

$$U_{sn} = i_{sn} r_{sn} + \frac{d\psi_{sn}}{dt} - \frac{d\psi_{smn}}{dt} + \frac{d\psi_{ssn}}{dt}, \quad \text{n=1, 2, 3, 4.} \tag{4}$$

Here, U_m, i_m, r_m, Ψ_m are the voltage, current, resistance and fluxes of the main winding, U_{sn}, i_{sn}, r_{sn}, Ψ_{sn} are the voltage, current, resistance and fluxes of the radial-force wind, Ψ_{msn}, Ψ_{smn} are the mutual fluxes between the main winding and the radial-force winding. Ψ_{ssn} are the mutual fluxes of the radial-force winding. According to the assumption, Ψ_{msn}, Ψ_{smn} and Ψ_{ssn} could be ignored. The voltage equations can be simplified as,

$$U_{sn} = \frac{d\Psi_{sn}}{dt} - \frac{d\Psi_{mn}}{dt} = \frac{dL_{sn} i_s}{dt} - \frac{dMi_m}{dt} \tag{5}$$

where L_{sn} is the self inductance of the radial-force windings, and M is the mutual inductance between the radial-force windings and the main windings.

Eq. (5) shows the current of the radial-force winding i_s can be calculated from L_{sn}, M and i_m.

Similarly, the voltage equation of the main winding (3) could become as follows:

$$\begin{aligned} U_m &= L_m \frac{di_m}{dt} + i_m \frac{\partial L_m}{\partial \theta}\omega + M \frac{d(i_{s1}+i_{s2}+i_{s3}+i_{s4})}{dt} + \omega \frac{\partial M}{\partial \theta}(i_{s1}+i_{s2}+i_{s3}+i_{s4}) \\ &= L_m \frac{di_m}{dt} + i_m \frac{\partial L_m}{\partial \theta}\omega + M \frac{d(i_{s1}+i_{s2}+i_{s3}+i_{s4})}{dt} + \omega \frac{\partial M}{\partial \theta}(i_{s1}+i_{s2}+i_{s3}+i_{s4}). \end{aligned} \tag{6}$$

The power circuit of the main winding is a rectifier bridge. Four coils of each phase are connected in series.

Simulation Results

The current waveforms can be derived by using the voltage Eq. (3) and Eq. (4). The validity of simulation model is tested and verified through the derived waveforms without considering levitation force as shown in Fig.9. The excitation voltage is 80V, the speed is 6000 r/min and the chopper current is 3A.

Fig.10 shows the experimental current waveforms. It is presented to prove the accuracy of the model.

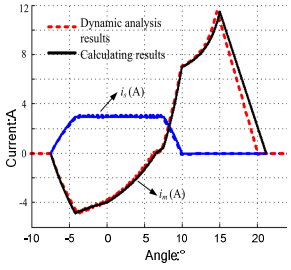

Fig.9 The simulation waveforms and derived waveforms

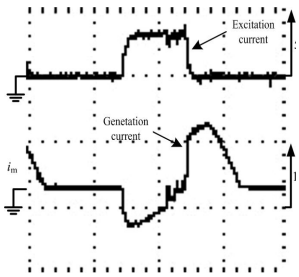

Fig.10 The experimental waveforms

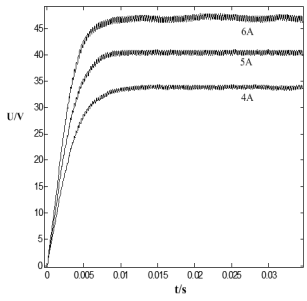

Fig.11 The influence of chopper current on output voltage

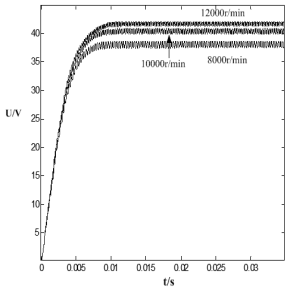

Fig.12 The influence of speed on output voltage

The model is simulated to analyze the influence of chopper current and speed on output voltage as shown in Fig.11 and Fig.12. The excitation voltage is 150V, the speed is 6000 r/min and the load is 2.5Ω. The output voltage rises when the chopper current increases. But the increment of chopper current causes the voltage ripple larger. Fig.14 shows speeding-up could increase the output voltage and reduce the voltage ripple.

Fig.13 shows the relationships between the radial forces and winding currents. When there is no levitation force in α-direction or β-direction, the radial-force winding currents coincide to that when $\triangle i_{s1}$ and $\triangle i_{s2}$ are zero in Eq. (1) and Eq. (2). The levitation force impacts on the winding currents, but the average value of the radial-force winding currents is constant equal to the average current i_s*, Eq. (6) could be written as,

$$U_m = L_m \frac{di_m}{dt} + i_m \frac{\partial L_m}{\partial \theta}\omega + M\frac{d(i_{s1}+i_{s2}+i_{s3}+i_{s4})}{dt} + \omega\frac{\partial M}{\partial \theta}(i_{s1}+i_{s2}+i_{s3}+i_{s4})$$

$$= L_m \frac{di_m}{dt} + i_m \frac{\partial L_m}{\partial \theta}\omega + 4M\frac{di_s^*}{dt} + 4\omega\frac{\partial M}{\partial \theta}i_s^* \quad . \tag{7}$$

Eq. (7) shows radial force has no influence on the output voltage. It accords to the simulation results in Fig 14.

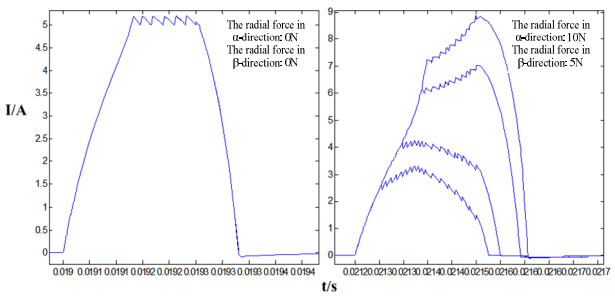

Fig.13 The influence of radial force on winding currents

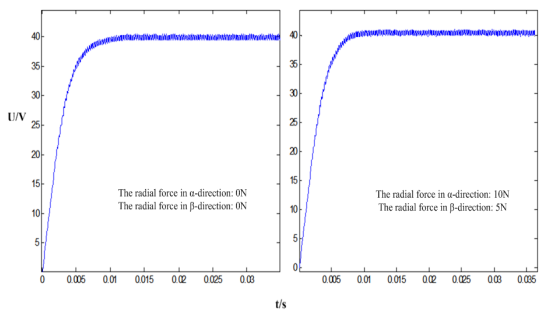

Fig.14 The influence of radial force on output voltage

Conclusion

In this paper, the linear simulation model of FPBSRG is established using relative blocks of MATLAB/SIMULINK. Then the model is simulated to analyze the characteristics of the motor. Relations between the radial forces and winding currents are studied from the simulation results. Radial force has no influence on the output voltage. The reason based is given on formula derivation.

Acknowledgements

This research was supported in part by Program for National Physical and Science Funds (50877036) and Graduate Innovative Base (Laboratory) Open Fund of Nanjing University of Aeronautics and Astronautics.

References

[1] A.Chiba, D.T.Power, M.A.Rahman: Characteristics of a Bearingless Induction Motor. IEEE Trans. 1991, 27(6): 5199-5201.
[2] M. Ohsawa, S. Mori, T. Satoh: Study of the Induction Type Bearingless Motor. 7th Int. Symp. Magnetic Bearings, ETH Zurich, Switzerland, 2000: 389-394.
[3] Xin Cao, Deng Zhiquan:A Full-period Generating Mode for Bearingless Switched Reluctance Generators. IEEE Trans, 2010, 20(3):1072-1076.